

## A QUADRATURE-RULE TYPE APPROXIMATION TO THE QUASI-CONTINUUM METHOD\*

MAX GUNZBURGER<sup>†</sup> AND YANZHI ZHANG<sup>†</sup>

**Abstract.** A quadrature-rule type approximation of the quasi-continuum method for atomistic mechanics is presented. Simple analysis and computational experiments are presented that illustrate that the new method has, for the same accuracy, lower complexity compared to not only the quasi-continuum method, but also to cluster-type approximations of that method. A discussion about some implementation issues connected to the new method is also provided.

**Key words.** quasi-continuum method, atomistic models, quadrature-rule type approximation, nanoindentation, Lennard-Jones potential

**AMS subject classifications.** 70C20, 70-08, 65N30, 65N15

**DOI.** 10.1137/080722151

**1. Introduction.** Atomistic simulations have become a prominent area of research, since many practical problems involve microscopic features such as dislocation and fracture phenomena [12, 20], nanoindentations [14, 17], atomic friction, and so on [14, 18, 21, 26]. Directly solving the whole system (molecular statics) provides an accurate solution for the analysis of microscopic features. However, the large number of atomistic particles in a material often makes it impossible to directly simulate the whole system. In addition, in many practical problems, defects occur only in some local and small regions where full atomistic resolution is needed. All these facts make it important to develop approximation or reduction methods for the original huge problem. The quasi-continuum (QC) method is one of the most successful multiscale techniques for reducing the complexity of large atomistic models. It combines continuum and atomistic descriptions in a rather seamless way, thus allowing for an efficient description of the system with accuracy comparable to that of the full atomistic model but at a much smaller cost.

Recently, many implementations, enhancements, extensions, and applications of the QC method are addressed in the literature [1, 2, 3, 5, 6, 7, 8, 9, 10, 13, 16, 18, 19, 22, 23, 25]. Analysis of the QC method and its variants can be found in, e.g., [2, 5, 7, 9, 10, 13, 16]. Although it has fewer degrees of freedom compared to the full atomistic model, the original QC method, in its raw form, still involves calculations over the full atomistic lattices so that the work needed to obtain a solution is still dependent on the total number of particles [13, 24, 25]. To avoid this, many studies are devoted to approximations to the QC method that result in a reduction in the computational complexity. The simplest approximate rule is the node-based summation rule [13, 24]. Although it reduces the computational cost of the QC method, in some cases it suffers from a rank-deficiency problem due to an insufficient number of sampling points. To overcome this problem, a cluster summation method (QC-CS), also known as the nonlocal QC method, was proposed in [13, 18]. If the QC-CS method is refined down

---

\*Received by the editors April 23, 2008; accepted for publication (in revised form) August 24, 2009; published electronically DATE. This work was supported by the U.S. Department of Energy under grant DE-FG02-05ER25698 as part of the Office of Science's "Multiscale Mathematics" program.

<http://www.siam.org/journals/mms/x-x/72215.html>

<sup>†</sup>Department of Scientific Computing, Florida State University, Tallahassee FL 32306-4120 (gunzburg@fsu.edu, yzhang5@fsu.edu).

to the atomic scale, it can exactly capture details of microscopic behavior. However, the QC-CS method requires the mapping of a cluster of atoms to their deformed configuration at every representative particle, which causes the calculation to depend on the cluster size. Thus, in practice, an optimal cluster size has to be determined to ensure the balance between computational complexity and numerical accuracy.

The aim of this paper is to present a cluster-independent approximation, namely, a quadrature-rule (QC-QR) type approximation, to the QC method. The paper is organized as follows. In section 2, we review the full atomistic and the QC methods for molecular statics and introduce the notations used in the following sections. In section 3, we present a detailed description of the QC-QR method and estimate its errors for a monoatomic chain. Some one-dimensional (1D) numerical experiments are provided in section 4 to test the QC-QR method and compare its performance to the QC and QC-CS methods. Finally, in section 5, we provide a brief summary and discussion of follow-up work.

## 2. QC method.

**2.1. Molecular statics.** We start with a brief review of the molecular statics model and notations used in the following sections. Let  $N$  denote the number of particles in a crystal and<sup>1</sup>  $\mathcal{N} = \{1, \dots, N\}$  denote the set of particle labels. In the reference configuration, these  $N$  particles occupy a subset of a simple  $d$ -dimensional ( $d = 1, 2$ , or  $3$ ) Bravais lattice. For  $\alpha \in \mathcal{N}$ , let  $\mathbf{X}_\alpha, \mathbf{x}_\alpha \in \mathbb{R}^d$  represent the (distinct) positions of the particle  $\alpha$  in the reference and in a deformed configuration, respectively. We denote by  $\Phi^a$  the potential energy of a configuration of particles due to the interaction between particles, and assume that  $\Phi^a$  is a function of the positions of all particles, i.e.,  $\Phi^a = \Phi^a(\{\mathbf{x}_\alpha\}_{\alpha \in \mathcal{N}})$ . In addition, the particles are subject to an external force field which we assume to be conservative and therefore derivable from an external potential function  $\Phi^e(\{\mathbf{x}_\alpha\}_{\alpha \in \mathcal{N}})$ . Then, the total potential energy  $\Phi$  is given by

$$(2.1) \quad \Phi(\{\mathbf{x}_\alpha\}_{\alpha \in \mathcal{N}}) = \Phi^a + \Phi^e.$$

We allow for the positions of some of the particles to be specified so that if  $\mathcal{N}_f \subset \mathcal{N}$  denotes the index set of the particles whose positions are specified, then

$$(2.2) \quad \mathbf{x}_\alpha = \mathbf{q}_\alpha \quad \text{for } \alpha \in \mathcal{N}_f$$

for given position vectors  $\mathbf{q}_\alpha$ ,  $\alpha \in \mathcal{N}_f$ . Let  $\mathcal{N}_a = \mathcal{N} \setminus \mathcal{N}_f$  so that  $\mathcal{N}_a$  is the set of indices of the remaining particles, i.e., those particles whose positions are not specified. Stable equilibrium positions of those particles are determined by minimizing the total energy,<sup>2</sup> subject to (2.2), i.e., by solving the problem

$$(2.3) \quad \min_{\mathbf{x}_\alpha, \alpha \in \mathcal{N}_a} \Phi(\{\mathbf{x}_\beta\}_{\beta \in \mathcal{N}}) \quad \text{subject to (2.2)}$$

or, equivalently,<sup>3</sup>

$$(2.4) \quad \frac{\partial \Phi}{\partial \mathbf{x}_\alpha}(\{\mathbf{x}_\beta\}_{\beta \in \mathcal{N}}) = \mathbf{0} \quad \text{for } \alpha \in \mathcal{N}_a \quad \text{and} \quad \mathbf{x}_\alpha = \mathbf{q}_\alpha \quad \text{for } \alpha \in \mathcal{N}_f.$$

<sup>1</sup>In this paper, calligraphic letters, e.g.,  $\mathcal{N}$ , represent index sets and the corresponding Roman letter, e.g.,  $N$ , defines its cardinality.

<sup>2</sup>In general, the aim is not simply to determine the absolute minimizer of  $\Phi(\{\mathbf{x}_\beta\}_{\beta \in \mathcal{N}})$ , but rather the set of metastable configurations of the crystal, which is physically more relevant.

<sup>3</sup>We use the notation  $\partial \Phi / \partial \mathbf{y}$  to denote the  $d$ -vector  $\nabla_{\mathbf{y}} \Phi$  having components  $\partial \Phi / \partial y_k$ ,  $k = 1, \dots, d$ .

After substituting the constraints imposed by (2.2), we see that (2.4) is a system of  $dN_a$  equations in the  $dN_a$  unknowns  $\mathbf{x}_\alpha$ ,  $\alpha \in \mathcal{N}_a$ .

**2.2. QC approximation.** The essence of the QC method is to replace (2.3) by a constrained minimization of  $\Phi(\{\mathbf{x}_\beta\}_{\beta \in \mathcal{N}})$  over a suitably chosen subset, i.e., the set of the *representative particles* [24, 25]. Let  $\tilde{\mathcal{N}}_r \subset \mathcal{N}$  denote the index set of the representative particles, and for  $j \in \tilde{\mathcal{N}}_r$ , let  $\mathbf{X}_j$  denote the distinct position of the representative particle  $j$  in the reference configuration. The selection of the representative particles is based on the local variation of the fields and was addressed in detail in [13]. Note that the representative particles are chosen from among the set of all particles, so it may be the case that some of the representative particles are chosen from among the particles whose positions are specified. In practice, all particles whose positions are fixed through (2.2) are chosen to be among the representative particles so that we have  $\mathcal{N}_f \subset \tilde{\mathcal{N}}_r$ . Then, denote by  $\mathcal{N}_r = \tilde{\mathcal{N}}_r \setminus \mathcal{N}_f$  the set of indices of the remaining representative particles, i.e., those representative particles whose positions are not specified by (2.2).

Let  $\mathbf{T}_h = \{\Delta_t\}_{t=1}^T$  denote a triangulation (into simplices) having the representative particles serving as vertices. Note that this triangulation is constructed using the particle positions in the reference configuration. We let  $\mathbf{T}_{h,j} = \{\Delta_t \mid \mathbf{X}_j \in \overline{\Delta_t}\}$  denote the set of simplices which have the point  $\mathbf{X}_j$  as a vertex. Let  $\{\psi_j^h(\mathbf{X})\}_{j \in \tilde{\mathcal{N}}_r}$  denote a basis for the space of continuous, piecewise linear polynomials corresponding to the triangulation  $\mathbf{T}_h$ . In particular, we choose this basis so that

$$\psi_j^h(\mathbf{X}_i) = \begin{cases} 1 & i = j \\ 0 & i \neq j \end{cases} \quad \text{for } i, j \in \tilde{\mathcal{N}}_r.$$

In this case, we have that

$$\psi_j^h(\mathbf{X}) = 0 \quad \text{if } \mathbf{X} \in \overline{\Delta_t} \quad \text{but } \Delta_t \notin \mathbf{T}_{h,j}$$

so that the support of the basis function  $\psi_j^h(\mathbf{X})$  is limited to those simplices having  $\mathbf{X}_j$  as a vertex, i.e., to  $\mathbf{T}_{h,j}$ .

Based on the Cauchy–Born hypothesis, we assume that the position  $\mathbf{x}_\alpha$ ,  $\alpha \in \mathcal{N}_a$ , of the particles which are not fixed by (2.2) can be approximately determined from the (approximate) positions of the representative particles through interpolation, i.e., we have that

$$(2.5) \quad \mathbf{x}_\alpha^h = \sum_{j \in \tilde{\mathcal{N}}_r} \mathbf{x}_j^h \psi_j^h(\mathbf{X}_\alpha) \approx \mathbf{x}_\alpha \quad \text{for } \alpha \in \mathcal{N}_a,$$

where  $\mathbf{x}_j^h$  denotes the (approximate) position of the representative particle  $j$ . Note that (2.5) holds for all particles, including representative particles. Substituting (2.5) into (2.1), we obtain the approximation

$$(2.6) \quad \Phi^h(\{\mathbf{x}_j^h\}_{j \in \tilde{\mathcal{N}}_r}) = \Phi(\{\mathbf{x}_\alpha^h\}_{\alpha \in \mathcal{N}}) \approx \Phi(\{\mathbf{x}_\alpha\}_{\alpha \in \mathcal{N}})$$

to the total potential energy. Note that because of (2.5),  $\Phi^h$  is indeed a function of only the (approximate) positions  $\{\mathbf{x}_j^h\}_{j \in \tilde{\mathcal{N}}_r}$  of the representative particles. Thus, the only degrees of freedom appearing in  $\Phi^h$  are the approximate positions of the representative particles whose positions are not determined by (2.2). These degrees

of freedom are determined by solving the problem

$$(2.7) \quad \min_{\mathbf{x}_j^h, j \in \mathcal{N}_r} \Phi^h(\{\mathbf{x}_i^h\}_{i \in \tilde{\mathcal{N}}_r}) \quad \text{subject to (2.2)}$$

or, equivalently,

$$(2.8) \quad \begin{cases} \frac{\partial \Phi^h}{\partial \mathbf{x}_j^h}(\{\mathbf{x}_i^h\}_{i \in \tilde{\mathcal{N}}_r}) = \sum_{\alpha \in \mathcal{N}_a} \frac{\partial \Phi}{\partial \mathbf{x}_\alpha^h}(\{\mathbf{x}_\beta^h\}_{\beta \in \mathcal{N}}) \psi_j^h(\mathbf{X}_\alpha) = \mathbf{0} & \text{for } j \in \mathcal{N}_r, \\ \text{where } \mathbf{x}_\alpha^h = \mathbf{q}_\alpha & \text{for } \alpha \in \mathcal{N}_f \quad \text{and} \quad \mathbf{x}_\alpha^h = \sum_{j \in \tilde{\mathcal{N}}_r} \mathbf{x}_j^h \psi_j^h(\mathbf{X}_\alpha) & \text{for } \alpha \in \mathcal{N}_a. \end{cases}$$

We see that, after substituting the constraints imposed by (2.2) and (2.5), (2.8) is a system of  $dN_r$  equations in the  $dN_r$  unknowns  $\mathbf{x}_j^h$ ,  $j \in \mathcal{N}_r$ . In practice, we want to have that  $N_r \ll N_a$  so that the QC system (2.8) is much smaller than the exact molecular statics system (2.4).<sup>4</sup>

Let

$$\mathcal{N}_j = \{\alpha \in \mathcal{N}_a \mid \mathbf{X}_\alpha \in \text{supp}(\psi_j^h(\mathbf{X}))\},$$

i.e.,  $\mathcal{N}_j$  denotes the set of indices of the particles that, on the one hand, are located (in the reference configuration) within the support of the basis function  $\psi_j^h(\cdot)$  and, on the other hand, do not have their positions fixed by (2.2). Then, since

$$\psi_j^h(\mathbf{X}_\alpha) = 0 \quad \text{for } \alpha \in \mathcal{N}_a \setminus \mathcal{N}_j,$$

we have that (2.8) reduces to

$$(2.9) \quad \begin{cases} \sum_{\alpha \in \mathcal{N}_j} \frac{\partial \Phi}{\partial \mathbf{x}_\alpha^h}(\{\mathbf{x}_\beta^h\}_{\beta \in \mathcal{N}}) \psi_j^h(\mathbf{X}_\alpha) = \mathbf{0} & \text{for } j \in \mathcal{N}_r, \\ \text{where } \mathbf{x}_\alpha^h = \mathbf{q}_\alpha & \text{for } \alpha \in \mathcal{N}_f \quad \text{and} \quad \mathbf{x}_\alpha^h = \sum_{j \in \tilde{\mathcal{N}}_r} \mathbf{x}_j^h \psi_j^h(\mathbf{X}_\alpha) & \text{for } \alpha \in \mathcal{N}_a. \end{cases}$$

Even though (2.9) is a system of only  $dN_r$  equations in a like number of unknowns, the work involved in determining its solution still depends on  $N$ , the total number of particles. There are two causes that contribute to this work count:

1. The  $j$ th equation in (2.9) involves a sum over the particles located in the support of the basis function  $\psi_j^h(\mathbf{X})$ . Collectively, the number of summands that have to be evaluated in the system (2.9) is of the order  $O(N)$ .
2. Each summand itself is a function of  $N$  variables so that the evaluation of each summand requires work that depends on  $N$ .

---

<sup>4</sup>Note that we substituted the QC assumption (2.5) into the potential energy function to obtain (2.6) *before* we minimized the approximate potential energy in (2.7). We could have instead substituted (2.5) into (2.4), i.e., *after* the minimization of the exact potential energy in (2.3). Of course, the latter approach would lead to an overdetermined system of  $dN_a$  equations in  $dN_r$  unknowns. One would then be tempted to discard those equations corresponding to the particles whose positions are determined by the constraint (2.5), thus obtaining the system of  $dN_r$  equations in  $dN_r$  unknowns  $\frac{\partial \Phi}{\partial \mathbf{x}_j^h}(\mathbf{x}_1^h, \dots, \mathbf{x}_N^h) = \mathbf{0}$  for  $j \in \mathcal{N}_r$ . This set of equations does not properly account for the energy of the configuration; clearly, this system is different from the system (2.8).

Of course, we would like to further process the system (2.9) so as to obtain a system that can be solved in work depending on  $N_r$  but not on  $N$ .

On the other hand, even if the approximate positions  $\{\mathbf{x}_j^h\}_{j \in \mathcal{N}_r}$  of the representative particles are known, the evaluation of the corresponding approximate energy  $\Phi^h(\{\mathbf{x}_j^h\}_{j \in \tilde{\mathcal{N}}_r}) = \Phi(\{\mathbf{x}_\alpha^h\}_{\alpha \in \mathcal{N}})$  still requires work of complexity  $O(N^2)$ , since it is a function of the positions of all particles.

**2.3. Pairwise potentials and the corresponding forces.** We assume that the potential energy  $\Phi^a$  due to the interaction between particles is given as a sum of pairwise interaction potentials and that each of them depends only on the position of the corresponding pair of particles, i.e.,

$$(2.10) \quad \Phi^a(\{\mathbf{x}_\alpha\}_{\alpha \in \mathcal{N}}) = \frac{1}{2} \sum_{\alpha \in \mathcal{N}} \sum_{\beta \in \mathcal{N}, \beta \neq \alpha} \Phi_{\alpha, \beta}^a(\mathbf{x}_\alpha, \mathbf{x}_\beta),$$

where  $\Phi_{\alpha, \beta}^a(\mathbf{x}_\alpha, \mathbf{x}_\beta) = \Phi_{\beta, \alpha}^a(\mathbf{x}_\beta, \mathbf{x}_\alpha)$  denotes the potential energy due to the interaction between particle  $\alpha \in \mathcal{N}$  and particle  $\beta \in \mathcal{N}$  so that

$$\frac{\partial \Phi^a}{\partial \mathbf{x}_\alpha}(\{\mathbf{x}_\alpha\}_{\alpha \in \mathcal{N}}) = \sum_{\beta \in \mathcal{N}, \beta \neq \alpha} \frac{\partial \Phi_{\alpha, \beta}^a}{\partial \mathbf{x}_\alpha}(\mathbf{x}_\alpha, \mathbf{x}_\beta).$$

If we denote the force acting on particle  $\alpha$  due to the interaction with particle  $\beta$  by

$$\mathbf{f}_{\alpha, \beta}^a(\mathbf{x}_\alpha, \mathbf{x}_\beta) = -\frac{\partial \Phi_{\alpha, \beta}^a}{\partial \mathbf{x}_\alpha}(\mathbf{x}_\alpha, \mathbf{x}_\beta),$$

we then have

$$(2.11) \quad \frac{\partial \Phi^a}{\partial \mathbf{x}_\alpha}(\{\mathbf{x}_\alpha\}_{\alpha \in \mathcal{N}}) = - \sum_{\beta \in \mathcal{N}, \beta \neq \alpha} \mathbf{f}_{\alpha, \beta}^a(\mathbf{x}_\alpha, \mathbf{x}_\beta).$$

We also assume that the potential energy  $\Phi^e$  due to externally applied forces can be expressed as a sum of the potential energies of the forces acting on each particle and that the latter depends only on the position of the corresponding particle, i.e., we assume that

$$(2.12) \quad \Phi^e(\{\mathbf{x}_\alpha\}_{\alpha \in \mathcal{N}}) = \sum_{\alpha \in \mathcal{N}} \Phi_\alpha^e(\mathbf{x}_\alpha),$$

where  $\Phi_\alpha^e(\mathbf{x}_\alpha)$  denotes the potential energy on particle  $\alpha \in \mathcal{N}$  due to the external forces. We then have

$$(2.13) \quad \frac{\partial \Phi^e}{\partial \mathbf{x}_\alpha}(\{\mathbf{x}_\alpha\}_{\alpha \in \mathcal{N}}) = \frac{\partial \Phi_\alpha^e(\mathbf{x}_\alpha)}{\partial \mathbf{x}_\alpha} = -\mathbf{f}_\alpha^e(\mathbf{x}_\alpha)$$

with  $\mathbf{f}_\alpha^e(\mathbf{x}_\alpha)$  denoting the external force acting on particle  $\alpha \in \mathcal{N}$ .

Combining (2.9), (2.11), and (2.13) results in the force equilibrium equations

$$(2.14) \quad \begin{cases} \sum_{\alpha \in \mathcal{N}_j} \psi_j^h(\mathbf{X}_\alpha) \left( \sum_{\beta \in \mathcal{N}, \beta \neq \alpha} \mathbf{f}_{\alpha, \beta}^a(\mathbf{x}_\alpha^h, \mathbf{x}_\beta^h) \right) + \sum_{\alpha \in \mathcal{N}_j} \psi_j^h(\mathbf{X}_\alpha) \mathbf{f}_\alpha^e(\mathbf{x}_\alpha^h) = \mathbf{0} & \text{for } j \in \mathcal{N}_r, \\ \text{where } \mathbf{x}_\alpha^h = \mathbf{q}_\alpha & \text{for } \alpha \in \mathcal{N}_f \quad \text{and} \quad \mathbf{x}_\alpha^h = \sum_{j \in \tilde{\mathcal{N}}_r} \mathbf{x}_j^h \psi_j^h(\mathbf{X}_\alpha) & \text{for } \alpha \in \mathcal{N}_a. \end{cases}$$

It is now even more clear that the work involved in assembling the problem (2.9) depends on  $N$ . In (2.14), the inside summation over  $\beta \in \mathcal{N}$  involves a summation over  $N - 1$  particles. Moreover, for each  $j \in \mathcal{N}_r$ , the summations over  $\alpha \in \mathcal{N}_j$  involve summations over all the particles in the support of the basis function  $\psi_j^h(\cdot)$  so that, collectively, the work involved depends on  $\sum_{j \in \mathcal{N}_r} N_j$ , which is of the order of  $N$ .

Also note that, combining (2.6), (2.10), and (2.12), we have that the total potential energy is approximated by

$$(2.15) \quad \begin{cases} \Phi^h(\{\mathbf{x}_j^h\}_{j \in \tilde{\mathcal{N}}_r}) = \frac{1}{2} \sum_{\alpha \in \mathcal{N}} \sum_{\beta \in \mathcal{N}, \beta \neq \alpha} \Phi_{\alpha, \beta}^a(\mathbf{x}_\alpha^h, \mathbf{x}_\beta^h) + \sum_{\alpha \in \mathcal{N}} \Phi_\alpha^e(\mathbf{x}_\alpha^h), \\ \text{where } \mathbf{x}_\alpha^h = \mathbf{q}_\alpha \text{ for } \alpha \in \mathcal{N}_f \text{ and } \mathbf{x}_\alpha^h = \sum_{j \in \tilde{\mathcal{N}}_r} \mathbf{x}_j^h \psi_j^h(\mathbf{X}_\alpha) \text{ for } \alpha \in \mathcal{N}_a. \end{cases}$$

It is now also clear that the work involved in evaluating the approximate potential energy depends on  $N$  because of the sums with respect to both  $\alpha$  and  $\beta$ .

**2.4. Short-range interactions.** The interactions between particles are usually short-ranged, i.e., the magnitude of pairwise interaction potential decreases very fast when the distance between two particles becomes large. Thus, one common way to improve computational efficiency is to truncate the interatomic potential by assuming that the particle only interacts with its nearby particles and setting the interaction potential to be zero whenever the distance between two particles is larger than a cut-off radius  $r_c$ , i.e., for all  $\alpha, \beta \in \mathcal{N}$ ,

$$(2.16) \quad |\Phi_{\alpha, \beta}^a(\mathbf{x}_\alpha, \mathbf{x}_\beta)| = 0 \quad \text{whenever } |\mathbf{x}_\alpha - \mathbf{x}_\beta| > r_c.$$

In practice, to ensure both appropriate accuracy and computational efficiency, the cut-off radius  $r_c$  is chosen as, for a given prescribed tolerance  $\epsilon > 0$ ,

$$(2.17) \quad r_c = \min \hat{r} \quad \text{such that} \quad |\Phi_{\alpha, \beta}^a(\mathbf{x}_\alpha, \mathbf{x}_\beta)| < \epsilon \quad \forall r = |\mathbf{x}_\alpha - \mathbf{x}_\beta| > \hat{r}.$$

It is then safe to set  $\Phi_{\alpha, \beta}^a(\mathbf{x}_\alpha, \mathbf{x}_\beta) = 0$  outside of the cut-off region; see (2.16). In addition, it was suggested in [4] that a simple truncation may lead to a small discontinuity of energy at  $r = r_c$ . To avoid it, a simple “smoothing” term can be added to the potential so that both the interacting energy and its derivative, i.e., the interacting force, become zero at  $r = r_c$  [4].

Let

$$\mathcal{N}_{b(\alpha)} = \{\beta \in \mathcal{N} \mid 0 < |\mathbf{x}_\beta - \mathbf{x}_\alpha| \leq r_c\} \quad \text{for } \alpha \in \mathcal{N}$$

denote the index set of the particles interacting with the particle  $\alpha$ . Then, in the short-range interaction case, the approximate energy (2.15) reduces to

$$(2.18) \quad \begin{cases} \Phi^h(\{\mathbf{x}_j^h\}_{j \in \tilde{\mathcal{N}}_r}) = \frac{1}{2} \sum_{\alpha \in \mathcal{N}} \sum_{\beta \in \mathcal{N}_{b(\alpha)}} \Phi_{\alpha, \beta}^a(\mathbf{x}_\alpha^h, \mathbf{x}_\beta^h) + \sum_{\alpha \in \mathcal{N}} \Phi_\alpha^e(\mathbf{x}_\alpha^h), \\ \text{where } \mathbf{x}_\alpha^h = \mathbf{q}_\alpha \text{ for } \alpha \in \mathcal{N}_f \text{ and } \mathbf{x}_\alpha^h = \sum_{j \in \tilde{\mathcal{N}}_r} \mathbf{x}_j^h \psi_j^h(\mathbf{X}_\alpha) \text{ for } \alpha \in \mathcal{N}_a, \end{cases}$$

and the force equilibrium equations (2.14) become

(2.19)

$$\begin{cases} \sum_{\alpha \in \mathcal{N}_j} \psi_j^h(\mathbf{X}_\alpha) \left( \sum_{\beta \in \mathcal{N}_{b(\alpha)}} \mathbf{f}_{\alpha,\beta}^a(\mathbf{x}_\alpha^h, \mathbf{x}_\beta^h) \right) + \sum_{\alpha \in \mathcal{N}_j} \psi_j^h(\mathbf{X}_\alpha) \mathbf{f}_\alpha^e(\mathbf{x}_\alpha^h) = \mathbf{0} & \text{for } j \in \mathcal{N}_r, \\ \text{where } \mathbf{x}_\alpha^h = \mathbf{q}_\alpha & \text{for } \alpha \in \mathcal{N}_f \quad \text{and} \quad \mathbf{x}_\alpha^h = \sum_{j \in \tilde{\mathcal{N}}_r} \mathbf{x}_j^h \psi_j^h(\mathbf{X}_\alpha) & \text{for } \alpha \in \mathcal{N}_a. \end{cases}$$

Now in both (2.18) and (2.19), the inside summation over  $\beta \in \mathcal{N}_{b(\alpha)}$  involves a summation over the particles located inside of a small ball with center at the particle  $\alpha$  but no longer over all particles. Usually, for any  $\alpha \in \mathcal{N}$ , the number  $N_{b(\alpha)} \ll N$  and is independent of the total number of particles  $N$ . Consequently, the complexity in evaluating the total energy (2.18) and in solving equilibrium configuration (2.19) reduces to  $O(NN_b)$  with  $N_b$  the maximum number of particles in a ball, i.e.,  $N_b = \max_{\alpha \in \mathcal{N}} \{N_{b(\alpha)}\}$ .

**3. QC-QR type approximations.** It is easy to see from (2.18) and (2.19) that, even in the short-range interaction case, the application of the QC method cannot eliminate the dependence on the total number of particles  $N$ . This is caused by the outer summations which collectively or directly involve the calculation over all particles. To mitigate the causes for having work depending on  $N$ , in this section we approximate these summations by using “quadrature” rules.

**3.1. Quadrature rules.** There are two types of outer summations appearing in (2.18) and (2.19) that make the calculation depend on the total number of particles  $N$ . They have the following forms:

$$(3.1) \quad G = \sum_{\alpha \in \mathcal{N}} g(\mathbf{X}_\alpha) \quad \text{and} \quad G_j = \sum_{\alpha \in \mathcal{N}_j} g(\mathbf{X}_\alpha) \quad \text{for } j \in \mathcal{N}_r,$$

where  $g(\mathbf{X})$  is an appropriate function depending only on the position  $\mathbf{X}$ . To apply the quadrature rules, we first break up the sums in (3.1) into those over all representative particles  $\mathbf{X}_j$  ( $j \in \tilde{\mathcal{N}}_r$ ) and over all simplices  $\Delta_t$  ( $t = 1, \dots, T$ ). For each simplex  $\Delta_t$ , we denote by

$$\mathcal{N}_t = \{\alpha \in \mathcal{N} \text{ but } \alpha \notin \tilde{\mathcal{N}}_r \mid \mathbf{X}_\alpha \in \Delta_t\}$$

the index set of the particles located inside  $\Delta_t$ . As mentioned in section 2, all particles specified through (2.2) are to be among the representative particles, so we conclude that the particles whose indices belong to  $\mathcal{N}_t$  are not specified. If a particle is on the boundary between simplices but is not a representative particle, i.e., it is not located at a vertex, it can be arbitrarily assigned to one of the simplices. Also, let

$$\mathcal{T}_j = \{t \in \{1, \dots, T\} \mid \Delta_t \in \mathbf{T}_{h,j}\},$$

i.e.,  $\mathcal{T}_j$  denotes the index set of the simplices located inside of the support of the basis function  $\psi_j^h(\cdot)$ . Then, the two sums in (3.1) may be expressed in the form

$$(3.2) \quad \begin{aligned} G &= \sum_{t=1}^T \sum_{\alpha \in \mathcal{N}_t} g(\mathbf{X}_\alpha) + \sum_{k \in \tilde{\mathcal{N}}_r} g(\mathbf{X}_k), \\ G_j &= \sum_{t \in \mathcal{T}_j} \sum_{\alpha \in \mathcal{N}_t} g(\mathbf{X}_\alpha) + g(\mathbf{X}_j) \quad \text{for } j \in \mathcal{N}_r, \end{aligned}$$

respectively.

We now focus on the inside summations in (3.2), i.e., the sums over individual simplices. Our aim is to approximate the sum over all particles in a simplex by a (weighted) sum over fewer particles. To this end, for any simplex  $\Delta_t$  ( $t = 1, \dots, T$ ), we define the index set

$$(3.3) \quad \mathcal{N}_{t,q} = \begin{cases} \mathcal{N}_t & \text{if } N_t \leq q, \\ \text{a } q\text{-dimensional subset of } \mathcal{N}_t & \text{otherwise,} \end{cases}$$

i.e., in the latter case,  $\mathcal{N}_{t,q}$  consists of the indices of  $q$  particles chosen from among the particles in the simplex  $\Delta_t$ , where  $q$  depends on the “quadrature” rule we apply. Then, the sum over all particles in the simplex  $\Delta_t$  can be approximated by a weighted sum over the subset of particles whose indices belong to  $\mathcal{N}_{t,q}$ , i.e.,

$$(3.4) \quad \sum_{\alpha \in \mathcal{N}_t} g(\mathbf{X}_\alpha) \approx \sum_{\beta \in \mathcal{N}_{t,q}} \omega_{t,\beta} g(\mathbf{X}_\beta) \quad \text{for } t = 1, \dots, T,$$

where  $\mathbf{X}_\beta$  denotes the “quadrature” particles we choose in the simplex  $\Delta_t$  and  $\omega_{t,\beta}$  denotes the corresponding “quadrature” weights. The guidelines for selecting these particles and weights are addressed in section 3.2. Consequently, applying (3.4) to the sums in (3.2), we obtain

$$(3.5) \quad G \approx \sum_{t=1}^T \sum_{\beta \in \mathcal{N}_{t,q}} \omega_{t,\beta} g(\mathbf{X}_\beta) + \sum_{k \in \tilde{\mathcal{N}}_r} g(\mathbf{X}_k)$$

and

$$(3.6) \quad G_j \approx \sum_{t \in \mathcal{I}_j} \sum_{\beta \in \mathcal{N}_{t,q}} \omega_{t,\beta} g(\mathbf{X}_\beta) + g(\mathbf{X}_j) \quad \text{for } j \in \mathcal{N}_r.$$

It is easy to see that the complexity in computing sums (3.5) and (3.6) depends on the number of representative particles, the construction of the triangulation, and the quadrature rules employed, but it is independent of the total number of particles  $N$ .

**3.2. Quadrature particles and weights.** As defined in (3.3), if the number of particles in the simplex  $\Delta_t$  is less than or equal to  $q$ , then all of them are used in the summation (3.4), i.e.,  $\mathcal{N}_{t,q} = \mathcal{N}_t$ . Thus, in this case, the sum (3.4) is exact for any function  $g(\cdot)$ , and the weight  $\omega_{t,\beta} \equiv 1$  for  $\beta \in \mathcal{N}_{t,q}$ .

On the other hand, if the number of particles is larger than  $q$ , then only  $q$  of them are selected to be “quadrature” particles and used in (3.4). The basic requirement for selecting the quadrature points  $\mathbf{X}_\beta$  ( $\beta \in \mathcal{N}_{t,q}$ ) is that they are not coplanar, i.e., they do not lie on a  $(d-1)$ -dimensional plane. The noncoplanarity of these points is necessary for this system to be invertible. In addition, it is beneficial to choose these points so that the system is well conditioned. Since the triangulation  $\mathcal{T}_h$  is effected in the reference configuration of particles, it should be easy to choose points that satisfy this requirement. In practice, we can choose those particles nearest to some set of standard quadrature points for the simplex  $\Delta_t$ . In fact, if we were approximating integrals instead of sums, we would choose exactly those quadrature points in the simplex  $\Delta_t$ , but since we are approximating sums, we have no assurance that there are “quadrature” particles available at standard quadrature points for the simplex  $\Delta_t$ .

On each simplex  $\Delta_t$  ( $t = 1, \dots, T$ ), the weights  $\omega_{t,\beta}$  should be chosen to ensure that the approximation (3.4) is exact for a class of functions  $g(\cdot)$  [22], i.e., by solving



the system of  $q$  equations

$$(3.7) \quad \sum_{\beta \in \mathcal{N}_{t,q}} \omega_{t,\beta} g(\mathbf{X}_\beta) = \sum_{\alpha \in \mathcal{N}_t} g(\mathbf{X}_\alpha) \quad \text{for } \beta \in \mathcal{N}_{t,q}$$

in the  $q$  unknowns  $\omega_{t,\beta}$ . The weights  $\omega_{t,\beta}$  are not necessarily integers and may be regarded as the number of particles represented by the “quadrature” particles  $\mathbf{X}_\beta$ .

For example, in the reference configuration, we consider a 1D particle chain uniformly distributed on a straight line. In this case, the simplex  $\Delta_t \in \mathcal{T}_h$  is the interval between two representative particles, i.e.,  $\Delta_t = (X_j, X_{j+1})$ , with  $X_{j+1} > X_j$  and  $t = j = 1, \dots, \tilde{N}_r - 1$ . On each simplex, we use at most two quadrature particles, i.e., we set  $q = 2$  in (3.3). If a simplex  $\Delta_t$  has more than two particles, the quadrature particles can be chosen as

$$(3.8) \quad X_\beta = \arg \min_{\alpha \in \mathcal{N}_t} \left| X_\alpha - X_j - \frac{\beta L}{3} \right| \quad \text{for } \beta = 1, 2,$$

where  $L = X_{j+1} - X_j$  defines the size of the simplex, i.e., we choose two quadrature particles nearest to the  $1/3$  and  $2/3$  locations along the 1D simplex. Then, the weights can be calculated by requiring that (3.4) is exact for linear polynomials  $g(\cdot)$  so that we have the linear system

$$(3.9) \quad \omega_{t,1} + \omega_{t,2} = N_t \quad \text{and} \quad \omega_{t,1} X_1 + \omega_{t,2} X_2 = \sum_{\alpha \in \mathcal{N}_t} X_\alpha$$

for the two weights  $\omega_{t,1}$  and  $\omega_{t,2}$ .

In fine regions of the triangulation  $\mathcal{T}_h$ , the sums on the right-hand side of (3.7) may be computed explicitly. By contrast, in coarse regions where the mesh approaches the continuum limit, this explicit calculation becomes impractical. However, in such regions the sum reduces to an integral, and the corresponding weights are those of conventional Lobatto quadrature [11, 13]. In this limit, each simplex  $\Delta_t \in \mathcal{T}_h$  simply contributes  $(N/V)|\Delta_t|/q$  particles to each of its  $q$  quadrature points, where  $|\Delta_t|$  and  $V$  are the volumes of the simplex and the crystal in the reference configuration, respectively. Then  $N/V$  is the atom density of the crystal.

Note that the selection of the quadrature particles and the computation of their weights are done in the reference configuration so that they are independent of the actual positions of the particles. Thus, the same weights  $\omega_{t,\beta}$  and “quadrature” particles  $\mathbf{X}_\beta$  can be used throughout an iterative process that determines the solution of (2.19).

**3.3. Error analysis for a monoatomic chain.** In this subsection, we analyze the accuracy of the QC-QR method for a simple 1D monoatomic chain used in [13] and compare it with the QC-CS method. The index set is defined by  $\mathcal{N} \equiv \mathbb{Z}$ . In the reference configuration, we choose the distance between two neighboring particles to be  $h = 1$  so that the position of particles can be defined as  $X_\alpha = \alpha$  for  $\alpha \in \mathbb{Z}$ . For simplicity, a uniform triangulation of size  $L > 0$  is used. The coordinates of the representative particles are  $X_j = jL$  for  $j \in \tilde{\mathcal{N}}_r = \mathbb{Z}$ , and the simplex can be defined as  $\Delta_j = (X_j, X_{j+1})$ ; see Figure 3.1.

To obtain the summation error in the leading order, the sum of a quadratic polynomial supported only on two adjacent simplices in the reduced chain is considered, i.e.,

$$(3.10) \quad g(X) = \begin{cases} X^2 & X \in [-L, L], \\ 0 & \text{otherwise.} \end{cases}$$

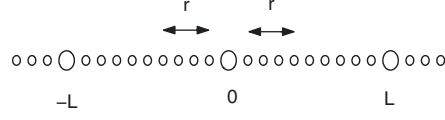


FIG. 3.1. A part of the 1D monoatomic chain with  $L = 10$ , where the “big” particles are representative particles and  $r$  is the radius of the clusters used in the QC-CS method.

It is easy to obtain the exact sum of  $g(X)$  over all sites of the chain, i.e.,

$$(3.11) \quad S = \sum_{\alpha \in \mathcal{N}} g(X_\alpha) = \sum_{\alpha=-L}^L (X_\alpha)^2 = \sum_{\alpha=-L}^L \alpha^2 = \frac{L(L+1)(2L+1)}{3}.$$

In the QC-QR method, we use two quadrature particles on each simplex. The quadrature particles and their weights can be computed by using (3.8) and (3.9). For example, on the simplex  $\Delta_t = (0, L)$ , we choose two points as

$$(3.12) \quad X_1 = \frac{L}{3}, \quad X_2 = \frac{2L}{3}.$$

Here we assume that these two points are exactly on the lattice sites, i.e., there exist particles on the two points. Then, from (3.9) and (3.12), we obtain the weights  $\omega_{t,1} = \omega_{t,2} = (L-1)/2$ , i.e., each quadrature particle represents  $(L-1)/2$  particles in this simplex. Thus, the approximate sum of the QC-QR method can be calculated by

$$(3.13) \quad \begin{aligned} S_{\text{QC-QR}}^h &= \sum_{t=1}^T \sum_{\beta=1}^2 \omega_{t,\beta} g(X_\beta) + \sum_{j \in \tilde{\mathcal{N}}_r} g(X_j) \\ &= \sum_{t=-1}^0 \sum_{\beta=1}^2 \omega_{t,\beta} g(X_\beta) + [g(-L) + g(0) + g(L)] = \frac{5L^3 + 13L^2}{9}, \end{aligned}$$

which depends only on the size of the simplex.

On the other hand, the use of the QC-CS method gives the approximation [13]

$$(3.14) \quad S_{\text{QC-CS}}^h = \frac{2(r+1)L}{3(2r+1)} [3L^2 + r(1-3L) + 2r^2]$$

with  $0 \leq r \leq L/2$  the radius of uniform clusters; see Figure 3.1.<sup>5</sup> In particular, if the radius  $r = 0$ , the approximate sum becomes

$$(3.15) \quad S_{\text{QC-CS}}^h|_{r=0} = 2L^3 = S_{\text{QC-NS}}^h,$$

where  $S_{\text{QC-NS}}^h$  is the approximate result of the node-based summation method (QC-NS) [13].

<sup>5</sup>Of course, we also could parameterize the QC-QR method by introducing “higher-order” quadrature rules that would require more quadrature particles in each simplex. However, as it is shown below, the “lowest-order” QC-QR method compares favorably with the QC-CS method for any practical choice of cluster size. Thus, it suffices for us to confine the discussion to the “lowest-order” QC-QR method.

From (3.11), (3.13), and (3.14), we can obtain the summation errors  $|S^h - S|$  of the QC-QR and QC-CS methods as

$$(3.16) \quad e_{\text{QC-QR}} = \left| \frac{1}{9}L^3 - \frac{4}{9}L^2 + \frac{1}{3}L \right|,$$

$$(3.17) \quad e_{\text{QC-CS}} = \left| \frac{2(r+2)}{3(2r+1)}L^3 - \frac{(2r^2+4r+1)}{(2r+1)}L^2 + \frac{(2r^2+2r-1)}{3}L \right|,$$

respectively. In the continuum region, i.e.,  $L \gg 1$ , we have that the leading order of the exact sum (3.11) is  $S \sim 2L^3/3$ . Thus, in this regime, the leading order of the relative error of the QC-QR method is given by

$$(3.18) \quad \tilde{e}_{\text{QC-QR}} = \frac{e_{\text{QC-QR}}}{S} \sim \frac{L^3/9}{2L^3/3} = \frac{1}{6},$$

which is a constant and independent of the simplex size  $L$ . On the other hand, the leading order of (3.17) depends on the radius of the clusters. So, to obtain the relative errors of the QC-CS method, we need divide our discussion into the following two cases.

*Case I*  $r \ll L$ . In this case, the leading order of (3.17) and its relative error become

$$(3.19) \quad e_{\text{QC-CS}} \sim \frac{2(r+2)}{3(2r+1)}L^3, \quad \tilde{e}_{\text{QC-CS}} \sim \frac{(r+2)}{(2r+1)} = \frac{1}{2} + \frac{3}{2(2r+1)} \geq \frac{1}{2},$$

respectively. This implies that the relative error of the QC-CS method depends on the radius of the clusters. For any radius  $r$ , the relative error is always larger than  $\frac{1}{2}$ ; in particular, it reaches the maximum value 2 when  $r = 0$ , i.e., for the case of the node-based summation rule. Thus, we can conclude that when  $L \gg 1$ , for any radius  $0 \leq r \ll L$  the QC-QR method has better accuracy than the QC-CS method. On the other hand, on each simplex, the QC-QR method uses only two quadrature particles, whereas the QC-CS method needs  $2r$  particles. Thus, if  $r > 1$ , the complexity of the QC-CS method is larger than that of the QC-QR method.

*Case II*  $r \sim O(L)$ . Assuming that  $r = cL$  with  $0 < c \leq \frac{1}{2}$ , we have the leading order of (3.17) and its relative error as

$$(3.20) \quad e_{\text{QC-CS}} \sim \frac{2c^2 - 3c + 1}{3}L^3, \quad \tilde{e}_{\text{QC-CS}} \sim \frac{2c^2 - 3c + 1}{2},$$

respectively. It is easy to see that when  $c = \frac{1}{2}$ , i.e.,  $r = L/2$ , the errors from the QC-CS method become 0. But, in this case, all the particles are used in the calculation, which does not reduce the complexity at all. Thus, we will only consider the case with  $c < \frac{1}{2}$ . By requiring that

$$\tilde{e}_{\text{QC-QR}} = \tilde{e}_{\text{QC-CS}} \quad \text{so that} \quad \frac{2c^2 - 3c + 1}{2} = \frac{1}{6},$$

we have

$$(3.21) \quad c = \frac{3}{4} - \frac{\sqrt{33}}{12} \approx 0.2713 \quad \text{so that} \quad r \approx 0.2713L.$$

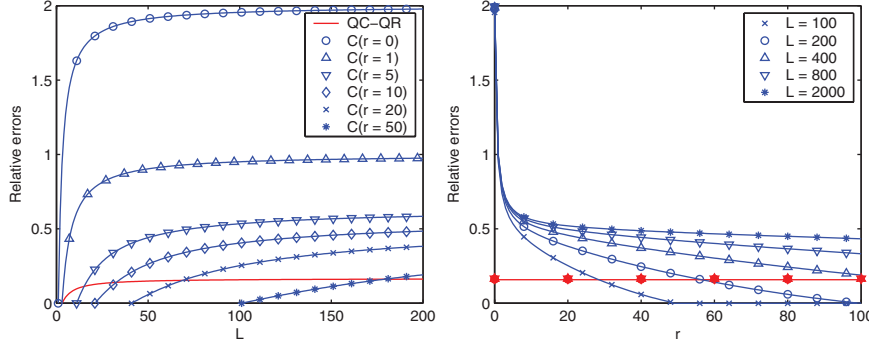


FIG. 3.2. The relative errors in computing the approximate sum for (3.11) versus the simplex size  $L$  (left) and the radius of clusters  $r$  (right), where “blue” is the QC-CS method; “red” is the QC-QR method.

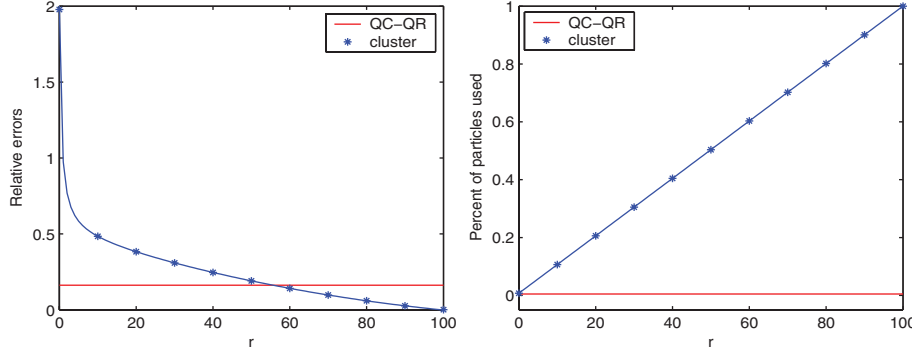


FIG. 3.3. For a fixed simplex size  $L = 200$ , the relative errors (left) and the percent of particles used in the calculation (right) versus the radius of clusters.

This implies that to obtain the same accuracy as that of the QC-QR method, in each simplex the QC-CS method has to use more than half of the particles.

Consequently, its complexity depends on the total number of particles.

Recall that the motivation for using either the QC-CS or QC-QR methods is to reduce the complexity of the original QC method, which depends on the total number of particles  $N$ . The QC-CS method with  $r \sim O(L)$  can get better accuracy than the case with  $r \ll L$ , but it does not essentially mitigate the dependence on the total number of particles in the calculation. Thus, in practice, only Case I with  $r \ll L$  is of interest.

In (3.18)–(3.21), we compare the errors of the QC-QR and QC-CS methods in the leading order. To make a further comparison, in Figures 3.2 and 3.3, we study the relationship between the full relative errors  $\tilde{e}_{\text{QC-CS}}$  and  $\tilde{e}_{\text{QC-QR}}$ , the simplex size  $L$ , and the radius  $r$  in the QC-CS method.

Figure 3.2 shows that when the size of the simplex becomes large, the relative error from the QC-QR method is almost a constant around  $1/6$ . By contrast, the error of the QC-CS method highly depends on the radius  $r$ . For a fixed  $L$ , the bigger the cluster radius  $0 \leq r \leq L/2$ , the smaller the error  $\tilde{e}_{\text{QC-CS}}$ . The relative error reaches its maximum and minimum values at  $r = 0$  and  $r = 1/2$ , respectively. On the other hand, for a fixed  $r$ , the bigger the simplex size  $L$ , the bigger the error  $\tilde{e}_{\text{QC-CS}}$ . The results shown in Fig. 3.2 confirms our analysis in the leading order.

In Figure 3.3, we plot the relative errors and the computational complexity (proportional to the number of particles used in the calculation) for the fixed simplex size  $L = 200$ . From it, we find that when  $r \approx 56$ , the QC-CS method has the same error as that of the QC-QR method, but it uses more than 56% of all particles. In contrast, the QC-QR method uses only less than 1% particles.

**3.4. Reduced equations based on quadrature rules.** As we have seen in section 2, in the short-range interaction case, the QC method can be formulated in two ways: the *energy-based* QC method, e.g., (2.18), and the *force-based* QC method, e.g., (2.19). Both of them begin from the energy (2.6) and can be used to find the stable configurations of the particles. In this subsection, we give the formulation of the energy-based QC-QR method and the force-based QC-QR method by applying the quadrature rules to (2.18) and (2.19), respectively.

**3.4.1. Energy-based QC-QR method.** Applying (3.5) to (2.18), we obtain the approximate potential energy by the QC-QR method as

$$(3.22) \quad \left\{ \begin{array}{l} \Phi^h(\{\mathbf{x}_j^h\}_{j \in \tilde{\mathcal{N}}_r}) \approx \sum_{t=1}^T \sum_{\alpha \in \mathcal{N}_{t,q}} w_{t,\alpha} \left( \sum_{\beta \in \mathcal{N}_{b(\alpha)}} \frac{\Phi_{\alpha,\beta}^a(\mathbf{x}_\alpha^h, \mathbf{x}_\beta^h)}{2} + \Phi_\alpha^e(\mathbf{x}_\alpha^h) \right) \\ \quad + \sum_{k \in \tilde{\mathcal{N}}_r} \left( \sum_{\beta \in \mathcal{N}_{b(k)}} \frac{\Phi_{k,\beta}^a(\mathbf{x}_k^h, \mathbf{x}_\beta^h)}{2} + \Phi_k^e(\mathbf{x}_k^h) \right), \\ \text{where } \mathbf{x}_\alpha^h = \mathbf{q}_\alpha \text{ if } \alpha \in \mathcal{N}_f \text{ and } \mathbf{x}_\alpha^h = \sum_{k \in \tilde{\mathcal{N}}_r} \mathbf{x}_k^h \psi_k^h(\mathbf{X}_\alpha) \text{ if } \alpha \in \mathcal{N}_a. \end{array} \right.$$

As mentioned previously, the inner summations in (3.22) have the complexity of  $O(N_b)$ , which is independent of the total number of particles  $N$ , and the outer sums involve at most  $qT + \tilde{N}_r$  particles with  $T$  the total number of simplices. Consequently, the total work in evaluating the approximate energy (3.22) is of the order  $O((qT + \tilde{N}_r)N_b)$ , which is independent of the total number of particles  $N$ .

Similarly, to minimize the energy (3.22), we can solve for the force equilibrium equations to ensure that the total force on each degree of freedom is zero. Thus, differentiating (3.22) with respect to  $\mathbf{x}_j^h$  for  $j \in \mathcal{N}_r$ , we obtain that the force equilibrium equations corresponding to (3.22) are

$$(3.23) \quad \left\{ \begin{array}{l} \sum_{t \in \mathcal{T}_j} \sum_{\alpha \in \mathcal{N}_{t,q}} w_{t,\alpha} \psi_j^h(\mathbf{X}_\alpha) \left( \sum_{\beta \in \mathcal{N}_{b(\alpha)}} \frac{\mathbf{f}_{\alpha,\beta}^a(\mathbf{x}_\alpha^h, \mathbf{x}_\beta^h)}{2} + \mathbf{f}_\alpha^e(\mathbf{x}_\alpha^h) \right) \\ \quad + \left( \sum_{\beta \in \mathcal{N}_{b(j)}} \frac{\mathbf{f}_{j,\beta}^a(\mathbf{x}_j^h, \mathbf{x}_\beta^h)}{2} + \mathbf{f}_j^e(\mathbf{x}_j^h) \right) \\ \quad + \sum_{t=1}^T \sum_{\alpha \in \mathcal{N}_{t,q}} \omega_{t,\alpha} \sum_{\beta \in \mathcal{N}_j \cap \mathcal{N}_{b(\alpha)}} \psi_j^h(\mathbf{X}_\beta) \frac{\mathbf{f}_{\beta,\alpha}^a(\mathbf{x}_\beta^h, \mathbf{x}_\alpha^h)}{2} \\ \quad + \sum_{k \in \tilde{\mathcal{N}}_r} \sum_{\beta \in \mathcal{N}_j \cap \mathcal{N}_{b(k)}} \psi_j^h(\mathbf{X}_\beta) \frac{\mathbf{f}_{\beta,k}^a(\mathbf{x}_\beta^h, \mathbf{x}_k^h)}{2} = \mathbf{0} \quad \text{for } j \in \mathcal{N}_r, \\ \text{where } \mathbf{x}_\alpha^h = \mathbf{q}_\alpha \text{ if } \alpha \in \mathcal{N}_f \text{ and } \mathbf{x}_\alpha^h = \sum_{j \in \tilde{\mathcal{N}}_r} \mathbf{x}_j^h \psi_j^h(\mathbf{X}_\alpha) \text{ if } \alpha \in \mathcal{N}_a. \end{array} \right.$$

**3.4.2. Force-based QC-QR method.** In practice, instead of solving the explicit first-order necessary conditions corresponding to the energy function (3.22), i.e., solving the system (3.23), one usually works with the approximate force equations [13, 18]. To do this, we apply (3.6) to (2.19) to obtain

$$(3.24) \quad \left\{ \begin{array}{l} \sum_{t \in \mathcal{T}_j} \sum_{\alpha \in \mathcal{N}_{t,q}} w_{t,\alpha} \psi_j^h(\mathbf{X}_\alpha) \left( \sum_{\beta \in \mathcal{N}_{b(\alpha)}} \mathbf{f}_{\alpha,\beta}^a(\mathbf{x}_\alpha^h, \mathbf{x}_\beta^h) + \mathbf{f}_\alpha^e(\mathbf{x}_\alpha^h) \right) \\ \quad + \left( \sum_{\beta \in \mathcal{N}_{b(j)}} \mathbf{f}_{j,\beta}^a(\mathbf{x}_j^h, \mathbf{x}_\beta^h) + \mathbf{f}_j^e(\mathbf{x}_j^h) \right) = \mathbf{0} \quad \text{for } j \in \mathcal{N}_r, \\ \text{where } \mathbf{x}_\alpha^h = \mathbf{q}_\alpha \quad \text{if } \alpha \in \mathcal{N}_f \quad \text{and} \quad \mathbf{x}_\alpha^h = \sum_{j \in \tilde{\mathcal{N}}_r} \mathbf{x}_j^h \psi_j^h(\mathbf{X}_\alpha) \quad \text{if } \alpha \in \mathcal{N}_a. \end{array} \right.$$

For each  $j \in \mathcal{N}_r$ , the outer sums in the first line of (3.24) involve at most  $qT_j$  particles, where  $T_j$  is the number of simplices in the support of the basis function  $\psi_j^h(\cdot)$ . Thus collectively, the number of particles involved in the outer summations of all the equations in (3.24) is of the order of  $q \sum_{j \in \mathcal{N}_r} T_j + \tilde{N}_r$ ; this number is bounded independently of the total number of particles  $N$ .

For example, if a 1D particle chain is considered, then we have that  $T_j \leq 2$ . Thus, the number  $q \sum_{j \in \mathcal{N}_r} T_j + \tilde{N}_r$  is bounded by  $(2q+1)\tilde{N}_r$  so that the total computational complexity in solving the force equilibrium equations (3.24) is of the order  $O((2q+1)\tilde{N}_r N_b)$ , which is independent of the total number of particles  $N$ .

**4. Numerical tests.** In this section, we test the accuracy and efficiency of the QC-QR method by comparing it with the QC method, the QC-CS method, and the full atomistic method. The exact solution is chosen as that from the full atomistic method, and we measure the quality of the solutions in terms of both the energy and position. Then, the relative error in energy is defined by

$$(4.1) \quad E(\Phi) = \frac{|\Phi(\mathbf{x}) - \Phi^h(\mathbf{x}^h)|}{|\Phi(\mathbf{x})|},$$

where  $\mathbf{x}$  is the solution obtained from the full atomistic model,  $\mathbf{x}^h$  is the solution from approximate methods, e.g., the QC, QC-CS, or QC-QR methods. The position error is defined by

$$(4.2) \quad E_{L^2}(\mathbf{x}) = \|\mathbf{x} - \mathbf{x}^h\|_{L^2} = \sqrt{\frac{\sum (\mathbf{x} - \mathbf{x}^h)^2}{N}}.$$

In addition, we also define the displacement gradient  $F(\mathbf{X})$  as

$$(4.3) \quad F(\mathbf{X}) = \frac{d\mathbf{x}}{d\mathbf{X}} = \mathbf{I} + \frac{d\mathbf{u}}{d\mathbf{X}},$$

where  $\mathbf{I}$  is the identity tensor and  $\mathbf{u}(\mathbf{X}) = \mathbf{x} - \mathbf{X}$  is the displacement of the particles.

The simulations of the approximate methods as well as the full atomistic method require the use of an iterative method to solve the associated nonlinear systems. We purposely use very tight tolerances for the iterative method so that any error resulting from the iterative solver is negligible compared to the differences between the full

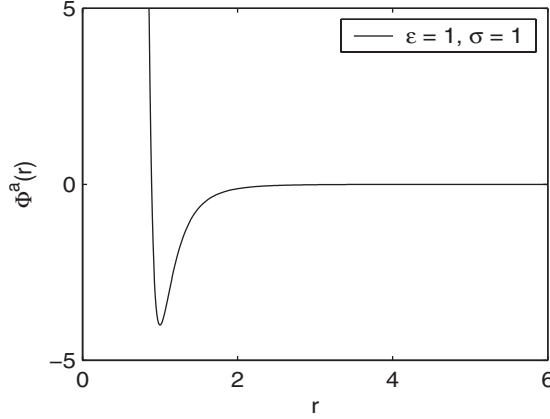


FIG. 4.1. *The Lennard-Jones potential as a function of the distance between two particles.*

atomistic and the approximate solutions. Thus, the sources of the errors we report on are due to the following: (i) for the QC, QC-CS, and QC-QR simulations, the error introduced because of the reduction of the number of degrees of freedom from  $N_a$  to  $N_r$  through the use of the Cauchy–Born hypothesis and the use of representative atoms, and (ii) for the QC-CS and QC-QR simulations, an additional error due to the use of the cluster or the quadrature-rule type approximations, respectively, for the sums in the QC model.

**4.1. Test problem definition.** We consider a simple 1D model of a crystalline material where all particles are distributed on a straight line. A “nanoindentation” is used to assess the performance of the methods [13]. This problem can present a highly nonuniform state of deformation, resulting in a lattice gradation away from the indenter.

In our examples, the popular 6–12 Lennard-Jones (LJ) potential is used, which takes the form [13, 15]

$$(4.4) \quad \Phi^a(r) = 4\epsilon \left[ \left( \frac{\sigma}{r} \right)^{12} - 2 \left( \frac{\sigma}{r} \right)^6 \right],$$

where  $r$  is the distance between two particles,  $\epsilon$  is a parameter determining the depth of the potential well, and  $\sigma$  is a length scale that determines the position of the minimum. In the following computations, we choose  $\epsilon = 1$  and  $\sigma = 1$ , and the shape of the LJ potential is shown in Figure 4.1.

A 1D nanoindenter is applied as an additional external potential  $\Phi^e(x)$  interacting with atoms; specifically, it has the form [12, 13]

$$(4.5) \quad \Phi^e(x) = \begin{cases} A(R - x)^2 & \text{if } R \geq x, \\ 0 & \text{otherwise,} \end{cases}$$

where  $R > 0$  is the radius of the indenter and  $A$  is a force constant. The parameters are chosen as  $A = 0.001$  and  $R = 100$ .

In the simulations, we consider a system with  $N = 2049$  particles which, in the reference configuration, are uniformly distributed on a straight line with an interparticle distance  $h$ . The two end-particles are fixed by setting  $x_0 = 0$  and  $x_{2048} = 2048h$  throughout the tests. Unless otherwise stated, the atomistic distance is set as  $h = 1$ ,

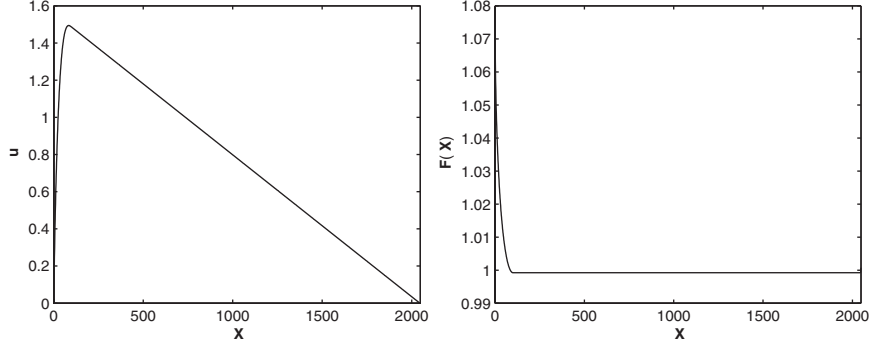


FIG. 4.2. The displacement  $u(X)$  (left) and the displacement gradient  $F(X)$  (right) of the particle chain.

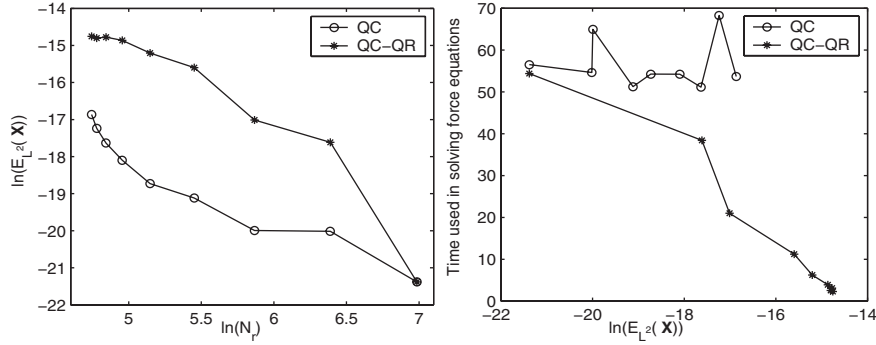


FIG. 4.3. The position errors of the QC and QC-QR methods versus the number of the representative particles (left) and the time used in solving the force equilibrium equations versus error values (right).

and no displacement constraints are applied to other particles. A cut-off radius  $r_c = 66$  in (2.17) is chosen by requiring that  $\epsilon = 10^{-10}$ .

Figure 4.2 shows the displacement of the particles  $u(X)$  and the displacement gradient  $F(X)$  for this example. In the region of  $[0, 100]$ , the chain has a high nonuniform deformation whereas for  $X > 100$ , the deformation is almost linear. Thus, in the computation, we use full atomistic resolution on  $[0, 100]$ , i.e., all the particles in this region are chosen to be the representative particles. For the region of  $[100, 2048]$ , a coarser mesh is used by choosing uniformly distributed representative particles.

**4.2. Accuracy of the force-based QC-QR method.** We numerically assess the rate at which the QC and QC-QR solutions converge toward the full atomistic solutions. Figure 4.3 provides the position errors of the QC and QC-QR methods for a different number of representative particles and also shows the time used in solving the force equilibrium equations versus the resulting error obtained. Similarly, Figure 4.4 displays the relative energy errors and the time consumed in evaluating the total potential energy.

From Figure 4.3 (left), we see that the errors of both the QC and QC-QR methods decrease when more representative particles are used in the simulation. The error of the QC-QR method is usually larger than that of the QC method, due to the extra errors introduced by using of the quadrature-type rule. However, the time used by the



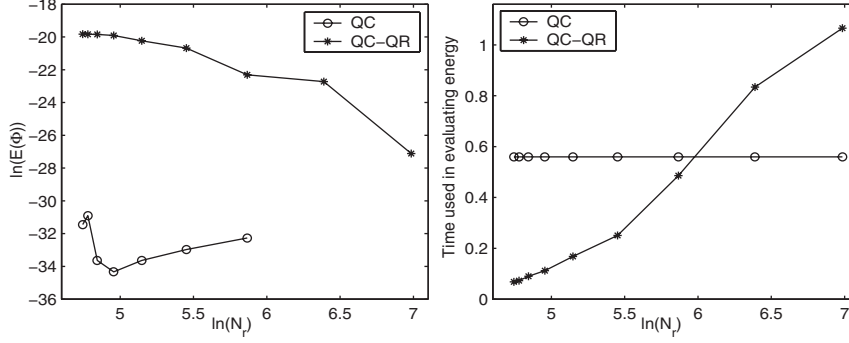


FIG. 4.4. The energy errors of the QC and QC-QR methods (left) and the time used in evaluating the approximate energy (right) versus the number of the representative particles.

QC-QR method is much shorter than that of the QC method. For example, Figure 4.3 (right) shows that for a given error level, the QC method needs more time to solve the force equilibrium equations. Furthermore, its time is insensitive to changes in the number of the representative particles, e.g., the time is always around 55. This is due to the fact that the costs associated with the QC method are dominated by the summations over all particles. On the other hand, having fewer representative particles can save a lot of time in the QC-QR method, since its complexity depends on the number of representative particles but not on the total number of particles.

Similarly, Figure 4.4 displays the relative errors and the time needed to determine the approximate energy. From that figure, we again observe that a decrease in the number of representative particles does not shorten the time spent by the QC method, whereas the time used by the QC-QR method is significantly reduced. Note that when  $\ln(N_r) \approx 6.2$ , i.e.,  $N_r \approx 500$ , the time used by the QC-QR method becomes larger than that of the QC method because, in this case, the simplices are quite small and almost every particle is used in the QC-QR method. Thus, in this case, the QC-QR method is equivalent to the QC method, but it has more overhead such as determining the quadrature particles in the computation. This suggests that the QC-QR method is more efficient for coarse meshes.<sup>6</sup>

**4.3. Comparison of the QC-QR and QC-CS methods.** In this subsection, we compare the QC-QR and QC-CS methods. Figure 4.5 displays the position errors of the QC-QR method and the QC-CS method with different cluster size. In addition, it provides the percentage of particles used in the calculation.

It is easy to see that the accuracy of both the QC-QR and QC-CS methods increases when more representative particles are used. For the QC-CS method and a fixed number of representative particles, the error also decreases with increasing cluster size  $r$ . However, the error for the QC-CS method is always larger than that for the QC-QR method. This qualitatively confirms the error analysis in section 3.3.

In addition, for any fixed number of representative particles, if the radius of the cluster  $r = 1$ , the number of particles used in the QC-CS method is the same as that used in the QC-QR method. In this case, the two methods have the same

<sup>6</sup>The discussion in this paragraph is about evaluating the energy, assuming one has in hand the positions of the particles. One should keep in mind that in a calculation, one has to solve the force balance equations to determine those positions so that the results displayed in Figure 4.3 should be factored in when one examines the costs to evaluate the energy.

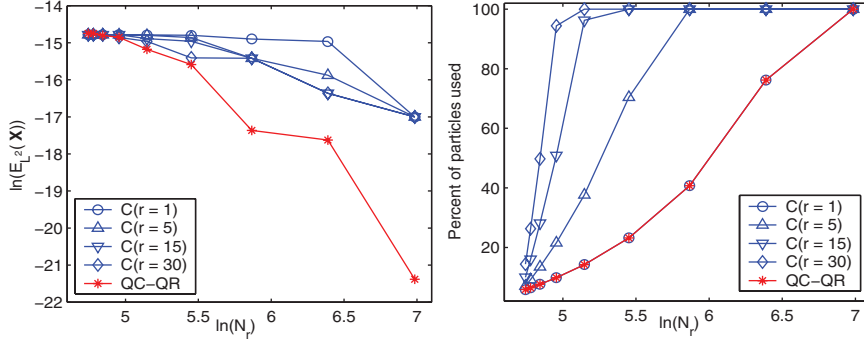


FIG. 4.5. The position errors of the QC-QR and QC-CS methods (left) and the percentage of particles used in calculations (right) versus the number of the representative particles.

TABLE 4.1

The relationship between the number of representative particles near the specified particle  $x_{2048}$ , the position error  $E_{L^2}(X)$ , and the relative energy error  $E(\Phi)$ .

Number of representative particles near $x_{2048}$	$E_{L^2}(X)$	$E(\Phi)$
0	9.3354E-4	9.4219E-6
1	1.4139E-4	1.0772E-6
2	3.3315E-5	3.3299E-7
5	1.5504E-6	9.7763E-9
10	2.5004E-7	1.3230E-9

computational complexity, but the QC-QR method is more accurate than the QC-CS method. For  $r > 1$ , the computational cost of the QC-CS method is always larger than that of the QC-QR method, as is the error.

**4.4. Representative particles near the specified particles.** As mentioned in section 2, in practice, all particles whose position are specified through (2.2) should be chosen to be among the representative particles. This is because the specified particles can be viewed as those having important information about the system, e.g., the boundary of the system as well as boundary values. From our simulations, we find that not only the specified particles but the particles near them should be taken as the representative particles in order to obtain good accuracy.

There are two specified particles in our example, i.e.,  $x_0$  and  $x_{2048}$ . Since all particles in the region  $[0, 100]$  have been selected as the representative particles, here we study only the effect of the representative particles near the particle  $x_{2048}$ . Table 4.1 provides the position errors  $E_{L^2}(X)$  and relative energy errors  $E(\Phi)$  for different numbers of representative particles near the specified particle  $x_{2048}$ . In this case, a uniform simplex size with  $N_t = 16$  is used in the region of  $[100, 2048]$ . It is easy to see that when more representative particles are used near to the specified particle  $x_{2048}$ , the errors in both position and energy decrease very fast.

**5. Summary and discussion.** We have presented a QC-QR type approximation to the QC method. Provided that the interatomic interaction is short-ranged, the QC method has a computational complexity of the order  $O(N)$ , with  $N$  the total number of particles, while the QC-QR method effectively reduces this complexity to

$O(\tilde{N}_r)$  so that its complexity depends only on the number of representative particles  $\tilde{N}_r$  with  $\tilde{N}_r \ll N$ .

We have presented some numerical tests to demonstrate the accuracy and performance of the QC-QR method. Compared to both the QC method and the QC-CS, the QC-QR method has substantially lower computational cost for the same accuracy. In addition, our numerical tests suggest that including more representative particles near the specified particles can highly improve the numerical accuracy.

There are several directions for further study. Certainly, one direction is to approximate the inner sums of (2.14) and (2.15) in cases involving long-ranged interatomic interactions. In such cases, we cannot truncate the potential into a small region so that the calculation involved in the inner sums still depends on the total number of particles  $N$ . However, there is the possibility of using quadrature-type rules for approximating the inner summations as well; this approach is being explored. Further analysis of the proposed method is also called for, following the lines of, e.g., [2, 5, 7, 9, 10, 16]. In addition, to further illustrate the usefulness of the method introduced in this paper, many additional computational tests are needed as is the use of the method to solve some application problems.

## REFERENCES

- [1] M. ARNDT AND M. LUSKIN, *Goal-oriented atomistic-continuum adaptivity for the quasicontinuum approximation*, Internat. J. Multi. Comput. Engrg., 5 (2007), pp. 407–415.
- [2] M. ARNDT AND M. LUSKIN, *Error estimation and atomistic-continuum adaptivity for the quasicontinuum approximation of a Frenkel–Kontorova model*, Multi. Model. Simul., 7 (2008), pp. 147–170.
- [3] M. ARNDT AND M. LUSKIN, *Goal-oriented adaptive mesh refinement for the quasicontinuum approximation of a Frenkel–Kontorova model*, Comput. Methods Appl. Mech. Engrg., 197 (2008), pp. 4298–4306.
- [4] V. BULATOV AND W. CAI, *Computer Simulations of Dislocations*, Oxford University Press, London, 2006.
- [5] M. DOBSON AND M. LUSKIN, *Analysis of a force-based quasicontinuum approximation*, M2AN Math. Model. Numer. Anal., 42 (2008), pp. 113–139.
- [6] M. DOBSON AND M. LUSKIN, *Iterative solution of the quasicontinuum equilibrium equations with continuation*, J. Sci. Comput., 37 (2008), pp. 19–41.
- [7] M. DOBSON AND M. LUSKIN, *An analysis of the effect of ghost force oscillation on quasicontinuum error*, M2AN Math. Model. Numer. Anal., 43 (2009), pp. 591–604.
- [8] M. DOBSON, M. LUSKIN, R. ELLIOTT, AND E. TADMOR, *A multilattice quasicontinuum for phase transforming materials: Cascading Cauchy Born kinematics*, J. Comput. Aided Mater. Des., 14 (2007), pp. 219–237.
- [9] W. E, J. LU, AND J. YANG, *Uniform accuracy of the quasicontinuum method*, Phys. Rev. B, 74 (2006).
- [10] W. E AND P. MING, *Analysis of the local quasicontinuum method*, in Frontiers and Prospects of Contemporary Applied Mathematics, Daqian Li, Tatsien Li, and Pingwen Zhang, eds., Higher Education Press, World Scientific, Singapore, 2005, pp. 18–32.
- [11] T. HUGHES, *The Finite Element Method: Linear Static and Dynamic Finite Element Analysis*, Prentice-Hall, Englewood Cliffs, NJ, 1987.
- [12] C. KELCHNER, S. PLIMPTON, AND J. HAMILTON, *Dislocation nucleation and defect structure during surface indentation*, Phys. Rev. B, 58 (1998), pp. 11085–11088.
- [13] J. KNAP AND M. ORTIZ, *An analysis of the quasicontinuum method*, J. Mech. Phys. Solids, 49 (2001), pp. 1899–1923.
- [14] J. KNAP AND M. ORTIZ, *Effect of indenter-radius size on Au(001) nanoidentation*, Phys. Rev. Lett., 90 (2003).
- [15] J. LENNARD-JONES AND A. DEVONSHIRE, *Critical and cooperative phenomena III. A theory of melting and the structure of liquids*, Proc. R. Soc. Lond. Ser. A Math. Phys. Eng. Sci., 169 (1939), pp. 317–338.
- [16] P. LIN, *Convergence analysis of a quasi-continuum approximation for a two-dimensional material without defects*, SIAM J. Numer. Anal., 45 (2007), pp. 313–332.

- [17] X-L. MA AND W. YANG, *Molecular dynamics simulation on burst and arrest of stacking faults in nanocrystalline Cu under nanoindentation*, Nanotechnology, 14 (2003), pp. 1208–1215.
- [18] R. MILLER AND E. TADMOR, *The quasicontinuum method: Overview, applications and current directions*, J. Comput. Aided Mater. Des., 9 (2002), pp. 203–239.
- [19] R. MILLER AND E. TADMOR, *Hybrid continuum mechanics and atomistic methods for simulating materials deformation and failure*, MRS Bull., 32 (2007), pp. 920–926.
- [20] R. MILLER, E. TADMOR, R. PHILLIPS, AND M. ORTIZ, *Quasicontinuum simulation of fracture at the atomic scale*, Model. Simul. Mater. Sci. Engrg., 6 (1998), pp. 607–638.
- [21] R. PHILLIPS, *Crystals, Defects and Microstructures: Modeling Across Scales*, Cambridge University Press, London, 2001.
- [22] V. SHENOY, R. MILLER, E. TADMOR, D. RODNEY, R. PHILLIPS, AND M. ORTIZ, *An adaptive finite element approach to atomic-scale mechanics: The quasicontinuum method*, J. Mech. Phys. Solids, 47 (1999), pp. 611–642.
- [23] E. TADMOR AND R. MILLER, *The theory and implementation of the quasicontinuum method*, in Handbook of Materials Modeling, Vol. 1, Kluwer Academic Publishers, Norwell, MA, 2005.
- [24] E. TADMOR, M. ORTIZ, AND R. PHILLIPS, *Quasicontinuum analysis of defects in solids*, Philos. Mag. A, 73 (1996), pp. 1529–1563.
- [25] E. TADMOR, R. PHILLIPS, AND M. ORTIZ, *Mixed atomistic and continuum models of deformation in solids*, Langmuir, 12 (1996), pp. 4529–4534.
- [26] M. TUCKERMAN AND G. MARTYNA, *Understanding modern molecular dynamics: Techniques and applications*, J. Phys. Chem. B, 104 (2000), pp. 159–178.